Süleyman Demirel Üniversitesi Fen Edebiyat Fakültesi Fen Dergisi https://dergipark.org.tr/sdufeffd
Süleyman Demirel University Faculty of Arts and Sciences Journal of Science e-ISSN: 1306-7575
Research Article, 2023, 18(2):181-194, DOI: 10.29233/sdufeffd.1220360

Benzotiyazolden Elde Edilen Bazı Azo Boyarmaddelerin Sentezi ve Yoğunluk Fonksiyonel Teorisi ile Analizi

Nesrin Şener*[1], M. Serdar Çavuş[2]

[1]Department of Chemistry, Faculty of Science, Kastamonu University, Kastamonu, *Turkey*
https://orcid.org/0000-0001-5370-6048
[2]Department of Biomedical Engineering, Faculty of Engineering and Architecture, Kastamonu University, Kastamonu, *Turkey*
https://orcid.org/0000-0002-3721-0883
**corresponding author: nsener@kastamonu.edu.tr*

(Alınış / Received: 17.12.2022, Kabul / Accepted: 12.05.2023, Yayımlanma / Published: 22.06.2023)

Abstract: In this study, two different azo dyes were synthesized from the reaction of 2-amino benzothiazole derivative amine and heterocyclic coupling compounds. The structures of the synthesized compounds were characterized such as by 1H-NMR and FT-IR spectroscopic methods. Four different possible tautomer structures are contemplated for each of the compounds. Considering the spectroscopic results analysis, the molecular structure of each tautomer was evaluated. UV-Vis. absorption properties of the obtained azo dyestuff compounds were studied using six different solvents. On the other hand, the electronic data of the spectroscopic and absorption properties of the tautomeric structures of the final products were examined theoretically at the B3LYP/6-311++G(2d,2p) theory level with the DFT approach. The experimental and theoretical results obtained in the study were compared with each other and the results were discussed.

Key words: Benzothiazole, DFT, heterocyclic, azo dyes.

Benzotiyazolden Elde Edilen Bazı Azo Boyarmaddelerin Sentezi ve Yoğunluk Fonksiyonel Teorisi ile Analizi

Öz: Yapılan bu çalışmada, 2-amino benzotiyazol türevi amin bileşikleri ve heterosiklik kenetleme bileşiğinin reaksiyonundan iki farklı azo boyarmadde sentezlenmiştir. Sentezlenen bileşiklerin molekül yapıları, ^{1}H-NMR ve FT-IR gibi spektroskopik yöntemlerle karakter analizine tabi tutulmuştur. Bileşiklerin her biri için muhtemel olan dört farklı tautomer yapı öngörülmüştür. Spektroskopik sonuç analizleri dikkate alınarak, herbir tautomer molekül yapısı değerlendirilmiştir. Elde edilen azo boyarmadde bileşiklerinin UV-Vis. absorpsiyon özellikleri altı farklı çözücü kullanılarak çalışılmıştır. Öte yandan elde edilen nihai ürünlerin tautomerik yapılarının spektroskopik ve absorpsiyon özelliklerinin elektronik verileri DFT yaklaşımıyla B3LYP/6-311++G(2d,2p) teori seviyesinde teorik olarak incelenmiştir. Çalışma sonucunda elde edilen deneysel ve teorik sonuçlar birbirleri ile karşılaştırılmış ve sonuçlar tartışılmıştır.

***Anahtar kelimeler**:* Benzotiyazol, DFT, heterosiklik, azo boyarmadde.

1. Introduction

Aromatic and heteroaromatic dyes are popular compounds that are widely used not only in textiles but also in other industrial fields [1-3]. Azo dyes containing aromatic moieties linked by azo chromophores are widely used in textile coloring such as polyester, nylon, acetate, cellulose and acrylic [4,5]. Azo dyes also having aromatic heterocycles are very

important because they have shown brilliant color and chromophoric strength, excellent light, color, washing and sublimation fastness as well as high level-dying property in the dyes industry. One of them, benzothiazole derivative azo dyes, is important in terms of being both red colored disperse dyes and cationic dyes. [6,7]. Benzothiazole derivative azo dyes compounds have been synthesized many times and the applications of these compounds in many different fields have been investigated [8]. It has also found a place in important application areas outside the textile field such as pharmacology [9], non-linear optical systems [10], anticancer activities [11] and antimicrobial activities [12].

Tautomerism, which has been known for over a century in azo dyes, is also an important issue in benzothiazole derivative azo dyes [8]. In particular, it was reported that Azo-hydrazone tautomerism is theoretically and practically attractive, and the two tautomers are from different cuisines [13]. It is understood from the literature that the comparison of experimental and theoretical results is very useful for evaluations in application areas [14,15]. For this reason, the synthesis of azo dyes compounds containing benzothiazole group and the theoretical calculations of these compounds by DFT method have been the subject of many studies in recent years [16-22].

Considering the diversity of usage areas as well as the interest on it, in this study, two different azo dyes were synthesized from the reaction of 2-amino benzothiazole derivative amine and heterocyclic coupling compounds. The structures of the synthesized compounds were characterized by 1H-NMR and FT-IR spectroscopic methods. The absorption properties of the compounds were also investigated using six different solvents. Moreover, the theoretical spectroscopy calculations of the compounds were performed using the DFT method and the results were compared with the experimental results. The possible tautomer structures of the compounds and their relations with the electronic parameters obtained from the calculations based on these structures were investigated. The conformations and spectral properties of the tautomer structures were also exanimated.

2. Material and Method

The chemicals and solvents (spectroscopic grade) used in this study were obtained from Aldrich (USA) and Merck Company (Germany) and were used without any purification. Melting points were recorded in the Electrothermal SMP30 device. Infrared spectra were recorded on the Bruker Alpha FTIR instrument. ^{1}H-NMR spectra were taken on Bruker (Germany) Spectrospin Avance DPX 400 Ultra-Shield spectrometer at room temperature by using tetramethylsilane (TMS) as the internal standard.

Compound 4-imino-3,4-dihydro-2H-pyrimido[2,1-b][1,3]benzothiazole-2-one was synthesized according to the literature [23].

2.1. Synthesis of (E)-4-imino-3-((6-methoxybenzo[d]thiazol-2-yl)diazenyl)-3,4-dihydro-2H-benzo[4,5]thiazolo[3,2-a]pyrimidin-2-one

2-Amino-6-methoxybenzothiazole compound (0.249 g and 1.38 mmol) was dissolved in 5 mL of acetic acid. $NaNO_2$ (0.095 g and 1.38 mmol) were dissolved in a minimum amount of H_2SO_4 by heating at 70 ºC and added dropwise in an amine solution cooled to 0-5 ºC. After 2 hours, the diazonium salt obtained from this solution was added to the 4-imino-3,4-dihydro-2H-pyrimido[2,1-b][1,3]benzothiazole-2-one (0.3 g and 1.38 mmol) in 10 mL of pyridine. The mixture was reacted at 0-5 °C for 2 hours. At the end of the reaction, it was precipitated by the addition of dilute sodium acetate. The resulting solid was filtered and dried. The dried solid was crystallized from a mixture of DMF/water (1:10). The reaction route is available in **Figure 1**.

This compound has been previously synthesized [24] in the literature and has been resynthesized with some solvent changes.

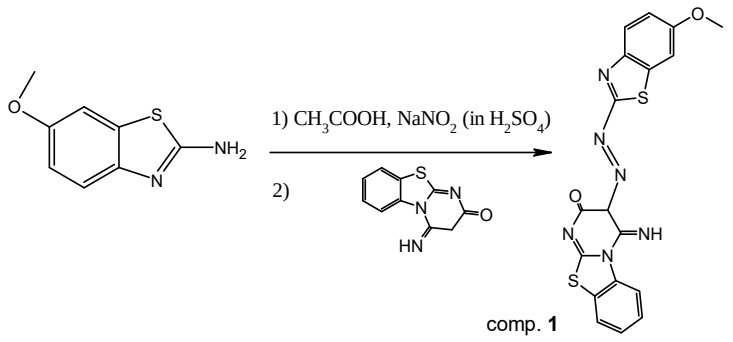

Figure 1. The reaction route of compound **1**.

2.2. Synthesis of (E)-4-imino-3-((5-(methylthio)-1H-1,2,4-triazol-3-yl)diazenyl)-3,4-dihydro-2H-benzo[4,5]thiazolo[3,2-a]pyrimidin-2-one

3-Amino-5-metil-tiyo-1H-1,3,4-triazol compound (0.179 g and 1.38 mmol) was dissolved in 10 mL acetic acid and 5 mL of HCl. $NaNO_2$ (0.095 g and 1.38 mmol) were dissolved in a minimum amount of H_2O and added dropwise in an amine solution cooled to 0-5 ºC. After 2 hours, the diazonium salt obtained from this solution was added to the 4-imino-3,4-dihydro-2H-pyrimido[2,1-b][1,3]benzothiazole-2-one (0.3 g and 1.38 mmol) in 10 mL of pyridine. The mixture was reacted at 0-5 °C for 2 hours. At the end of the reaction, it was precipitated by the addition of dilute sodium acetate. The resulting solid was filtered and dried. The dried solid was crystallized from a mixture of DMF/Water (1:10). The reaction route is available in **Figure 2**. Yield 68%, mp: 290 ºC, **ATR-FTIR (cm^{-1}) ν_{max}**: 3346.99 (-O-H stretching vibration), 3167.30 (=N-H bending vibration), 3058.36 (aromatic C-H stretching vibration), 2920.87, 2851.68 (aliphatic C-H stretching vibration), 1637.98 (C=C stretching vibration), 1584.16 (C=N stretching vibration), 747.68 (C-S-C stretching vibration). **^{1}H-NMR (δ, ppm, DMSO-d$_6$):** 2.75 (s, 3H –SCH_3), 7.34-8.08 (m, 4H aromatic CH), 8.82-9.16 (b, 1H –NH), 9.68 (s, 1H –OH), 12.45 (s, 1H =NH).

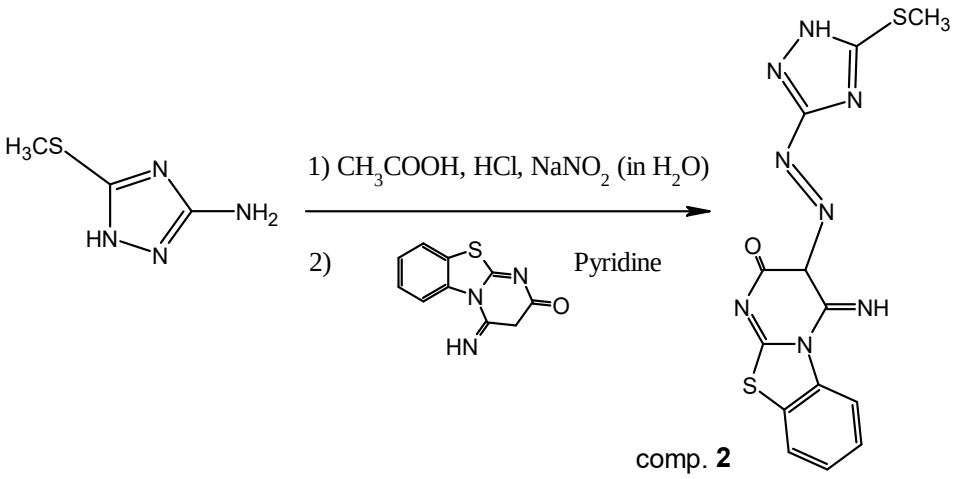

Figure 2. The reaction route of compound **2**.

2.3. UV-Vis. Absorption Study

The compounds synthesized in the UV-Vis absorption study were made using solutions prepared in six different solvents (Dimethylsulfoxide, *N*,*N*-Dimethylformamide, acetonitrile, methanol, chloroform and acetic acid) in the range of 300-700 nm at 10^{-4}-10^{-6} M concentration. The maximum absorbance values obtained for the two synthesized compounds were evaluated depending on the solvent change. The graphs obtained for compound **1** and compound **2** are shown in **Figure 3**.

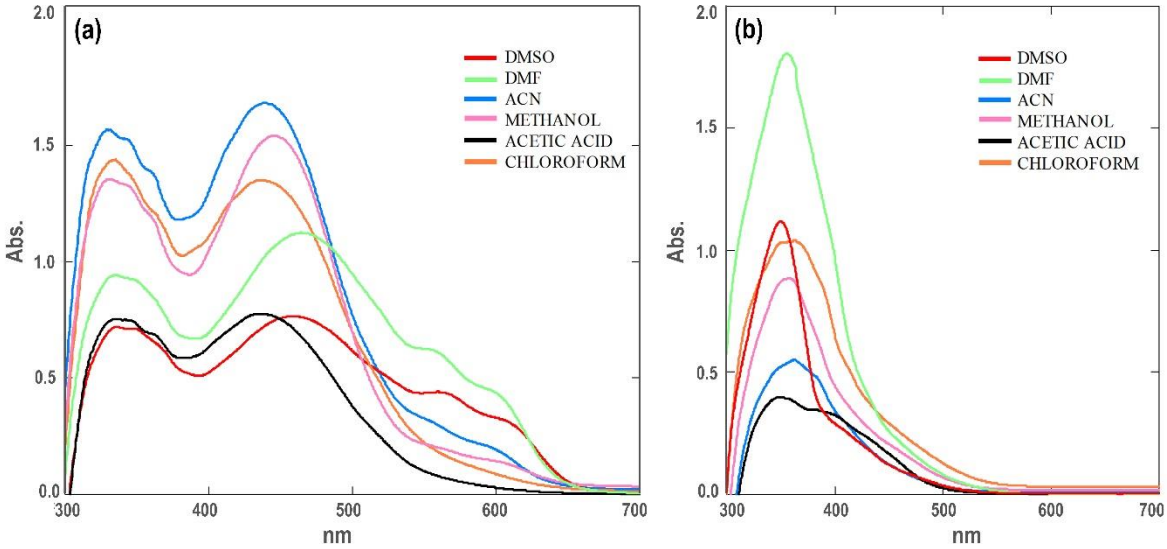

Figure 3. Absorption plots for compound 1 (a) and compound 2 (b) in different solvents.

2.4. Computational procedure

DFT [24, 25] calculations of the study were performed using Gaussian 09 software [26], with a basis set of 6-311++G(2d,2p) on the Becke 3-Parameter of Lee-Yang parr (B3LYP) functional. The IR calculations were completed successfully without any imaginary frequency mode performed in the gas phase and other calculation processes were started by checking that the compounds were optimized to the ground state energies corresponding to the minimum energy point on the potential energy surface. The frontier molecular orbital (FMO) energy eigenvalues of the compounds and global chemical reactivity parameters such as HOMO-LUMO band gap, chemical hardness, electronegativity, electrophilic index, nucleophilic index, electron donating and electron accepting powers were also obtained from the gas phase calculations at the same level of theory. QTAIM approach [27, 28] was used to analyze the changes of electron densities at bond critical points and ring critical points in tautomer structures. IRI [29] calculations were also performed to reveal the intramolecular interactions and the electron density of the bonds. Multiwfn software [30] was used for QTAIM and IRI analysis and data visualization.

Spectral calculations were also performed in the same solvent phases in accordance with the experiments at B3LYP/6-311++G(2d,2p) level of theory. ^{1}H NMR calculations were carried out in dimethyl sulfoxide (DMSO) phase with the solvent effect approach of the conductor-like polarizable continuum model (CPCM) using Gauge-independent atomic orbital (GIAO) method. The ^{1}H-NMR spectrum of tetramethylsilane (TMS) was calculated as 31.8149 ppm using the same level of theory, and the relative chemical shift values were obtained by subtracting the calculated absolute chemical shielding of TMS.

Time dependent DFT (TD-DFT) was used to calculate vertical excitation energies. UV spectral calculations were also performed at the same level, using the Self-Coherent Reaction Field (SCRF) method and CPCM approach, in accordance with the experiments,

in acetic acid, acetonitrile, dimethylformamide (DMF), dimethyl sulfoxide (DMSO), chloroform and methanol phases.

3. Results

Compound **1** was synthesized according to the literature [31] and the properties of the compound were found to be compatible with the literature. According to the ^{1}H-NMR analysis results of compound **2**, the peak belonging to the aliphatic group –SCH_3 protons in the structure is seen at 2.75 ppm. Aromatic protons in the structure are seen in the range of 7.34-8.08 ppm. While the peaks of two different –NH proton is widely seen in the range of 8.82-9.16 ppm, the peak of the –OH proton is observed at 9.68 ppm. Finally, the peak of the =NH proton is seen at 12.45 ppm. Integration rates of protons are compatible with the structure.

The maximum absorption results obtained compounds are shown in **Table 1**.

Table 1. The maximum absorption results of compounds **λ(nm)**

Compound	DMSO	DMF	ACN	Methanol	Acetic Acid	Chloroform
1	334, 349s, 458, 560s	334, 349s, 468, 555s	329, 342s, 360s, 440	330, 347s, 359s, 447	333, 345s, 363s, 437	335, 348s, 360s, 438
2	351, 404s	356	363, 383s	356, 403s	350, 390s	361, 349s, 388s

s: shoulder

For compound **1**, there appear to be two different maximum absorption points in all solvents in general. In addition, shouldering is observed at short and long wavelengths in all solvents except the solution of compound **2** in DMF. It is thus understood that the compounds have more than one tautomeric form in these solvents. It is generally observed that the maximum absorption points increase with the increase of the dielectric constant of the solvents. It is thought that the energy required for electronic transitions decreases with the increase in solvent polarity, and as a result, the absorbance value increases. For compound **2**, there is no such linear increase.

When the spectroscopic results are examined, it is observed that the solid state of the molecules and the states in the solution are different. For this reason, the structure is discussed over the different tautomeric forms of the molecules. Possible tautomeric forms of the structures of the compounds are given in **Figure 4** and **Figure 5**. When the spectroscopic analysis results are evaluated; Finding -C=O and -NH_2 stretching vibrations in the FT-IR and ^{1}H-NMR results [24] for compound **1** is thought to be in the **1Ta** tautomeric form of the structure in solid and solvent. For compound **2**, -OH and -NH stretching vibrations are found in the FT-IR and ^{1}H-NMR results, and the state of the structure in solid and solvent is considered to be in the **2Tb** tautomeric form. The regression analysis performed on the experimental data and the calculation results revealed that the results were compatible with each other. Such that, as a result of the regression analysis of the FT-IR data of compound **1** and its tautomeric form **1Ta**, $R^2 = 0.9932$ was calculated. Likewise, regression analysis for compound **2** and tautomeric form **2Tb** gave the result $R^2 = 0.9974$.

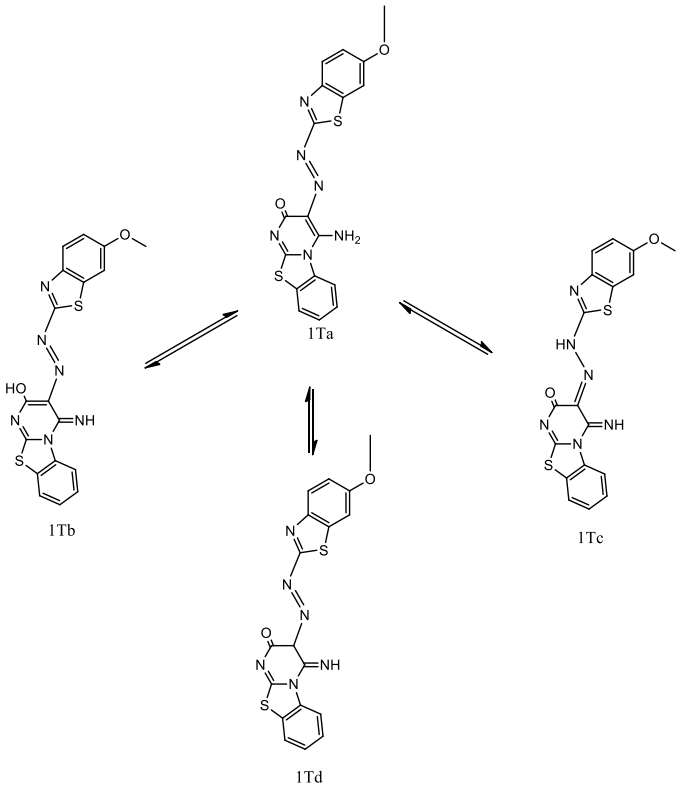

Figure 4. Possible tautomeric structures of compound **1**.

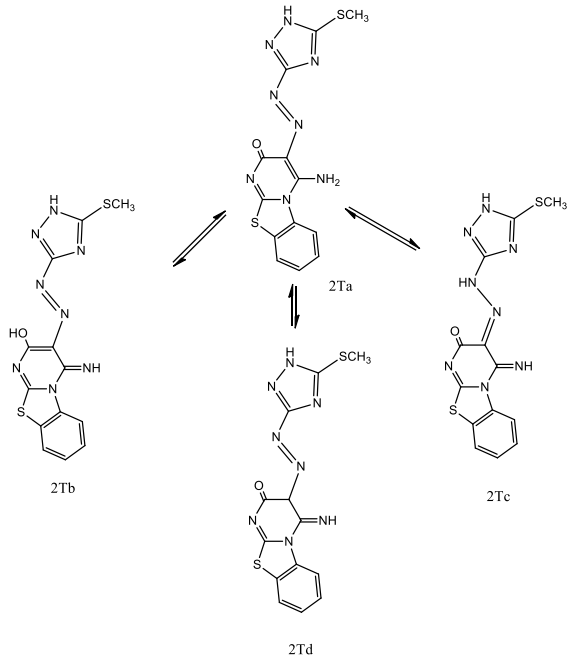

Figure 5. Possible tautomeric structures of compound **2**.

The calculated ^{1}H-NMR and IR data of the predicted tautomer forms of the compounds are given in **Table 2** and **Table 3**, respectively.

Table 2. Calculated ^{1}H-NMR data of the tautomers (ppm).

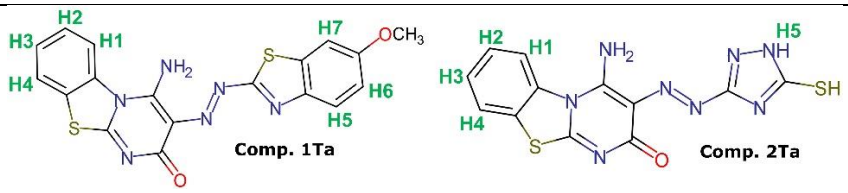

Isomer	H1	H2	H3	H4	NH2	NH	OH	=N-NH	Pyr. H	H5	H6	H7	CH3
1Ta	8.37	8.03	7.95	8.13	7.81, 5.59	-	-	-	-	8.23	7.41	7.68	4.25 - 3.96
1Tb	10.14	8.02	7.95	8.18	-	9.75	16.02	-	-	8.17	7.40	7.66	4.26 - 3.96
1Tc	9.84	7.92	7.84	8.04	-	10.32	-	15.71	-	8.04	7.39	7.67	4.24 - 3.93
1Td	9.17	7.93	7.84	8.05	-	10.12	-	-	5.59	8.48	7.54	7.73	4.29 - 4.01
2Ta	8.29	7.98	7.92	8.10	12.78. 6.72	-	-	-	-	10.01	-	-	3.09 , 2.47
2Tb	10.28	8.01	7.97	8.20	-	11.30	9.83	-	-	10.00	-	-	3.09 - 2.48
2Tc	9.85	7.91	7.85	8.02	-	10.19	-	15.52	-	9.79	-	-	3.08 - 2.48
2Td	9.08	7.89	7.84	8.03	-	9.32	-	-	8.09	10.32	-	-	3.14 - 2.52

Pyr. H: Pyrimidone H.

Table 3. Calculated IR data of the tautomers (cm^{-1}).

Isomer	NH2	NH	Tria. NH	=N-NH	OH	Ar.H	S/O-CH3	C=O	C=C	C=N	CSC
1Ta	3639a, 3520s	-	-	-	-	3220-3206	3142- 3016	1752	1637, 1622	1556	844, 732
1Tb	-	3512	-	-	2933	32611-319	3143-3017	-	1639, 1624	1566, 1537	848, 735
1Tc	-	3508	-	3236	-	3221-3193	3143-3015	1682	1640, 1624	1599, 1559	837, 742

1Td	-	3497	-	-	-	3253-3194	3146-3020	1781	1639, 1624	1589, 1582	847, 730
2Ta	3651a, 3218s	-	3651	-	-	3206-3195	3166 -3069	1758	1622,1607	1661	732
2Tb	-	3465	3653	-	3554	3259-3193	3169-3070	-	1624, 1612	1558	738
2Tc	-	3495	3664	3268	-	3262-3192	3170-3071	1659	1624, 1618	1557, 1528	735
2Td	-	3537	3645	-	-	3253-3193	3170-3071	1786	1624, 1618	1587, 1437	721

Tria: Triazol, Ar.H: Aromatic H, a: Asymetric stretching, s: Symetric stretching

3.1. DFT analysis

The compounds were handled in two groups, the first group tautomers **1T**(**a-d**) and the second group tautomers **2T**(**a-d**), and were examined both among themselves and mutually. Some global reactivity parameters calculated using FMOs are given in **Table 4**. The ability of a molecule to interact with the surrounding environment is related to its total dipole moment, and the calculated dipole moments for tautomers **1Ta** and **2Ta** are approximately 1.5-2 times greater than for other tautomers. These data indicate that tautomers **1Ta** and **2Ta** may show higher reactivity to interact with the surrounding environment. On the other hand, E_g is a crude but useful parameter for characterizing the chemical reactivity and kinetic stability of a molecule. It can be said that due to the highest E_g value of **1Td** and **2Td** in two groups of tautomer compounds, their reactivity is weaker and their kinetic stability is higher than other tautomers (see **Figure 6** for compound **1Ta** and **1Tb**). In this context, it is generally expected that the first group compounds will be more reactive than the second group compounds. In addition, while the HOMO energies of the first group tautomers were lower, the LUMO energies were calculated higher. A higher HOMO energy of a compound is directly related to its nucleophilic property, and a lower LUMO energy is related to its electrophilic behavior. Thus, in general, first group tautomers are expected to be more electrophilic than second group tautomers. The calculated electrophilic indices of the compounds also confirm such an expectation. The calculated ω values of the first group of tautomers ranged from 6.224 to 7.253 eV, while that of the second group of tautomers was calculated between 5.182-5.882 eV (see **Table 4**). In general, similar results were obtained for the nucleophilic indices of the compounds. In addition, both electron accepting and electron donating power values of the first group tautomers were higher than those of the second group. The polarizability of the first group tautomers was also calculated higher than the second group (in the range of 361,459-422.106 a.u for the first group, in the range of 276,850-310,863 a.u for the second group). The electronic data support the prediction that, overall for all tautomers, 2-amino-6-methoxy benzothiazole attached to pyrimidine makes the compounds more reactive than 3-amino-5-metil-tiyo-1H-1,3,4-triazol.

Table 4. Calculated electronic parameters of the compounds.

Isomer	E_{HOMO} (eV)	E_{LUMO} (eV)	E_g (eV)	η (eV)	χ (eV)	ω (eV)	ε (eV)	α *(au)*	μ *Debye*	ω^+ (eV)	ω^- (eV)
1Ta	-5.843	-2.825	3.018	1.509	4.334	6.224	3.652	405.366	11.744	1.322	5.656
1Tb	-5.778	-3.076	2.702	1.351	4.427	7.253	3.716	422.106	4.787	1.751	6.178

1Tc	-5.953	-3.105	2.848	1.424	4.529	7.202	3.542	392.756	5.520	1.693	6.221
1Td	-6.381	-2.955	3.426	1.713	4.668	6.359	3.114	361.459	5.465	1.274	5.942
2Ta	-6.099	-2.533	3.566	1.783	4.316	5.223	3.396	302.658	9.875	0.899	5.215
2Tb	-5.958	-2.630	3.329	1.664	4.294	5.540	3.536	310.863	2.200	1.039	5.333
2Tc	-6.221	-2.779	3.443	1.721	4.500	5.882	3.274	300.145	4.827	1.121	5.621
2Td	-6.541	-2.552	3.989	1.995	4.547	5.182	2.953	276.850	4.875	0.816	5.363

$\boldsymbol{E_g}$: $E_{LUMO} - E_{HOMO}$, $\boldsymbol{\eta}$: Chemical Hardness, $\boldsymbol{\chi}$: Electronegativity, **ω**: Electrophilic index, **ε**: Nucleophilic index, **α:** Polarizability, $\boldsymbol{\mu}$: Dipole moment, ω^+: electroaccepting power, ω^-: electrodonating power

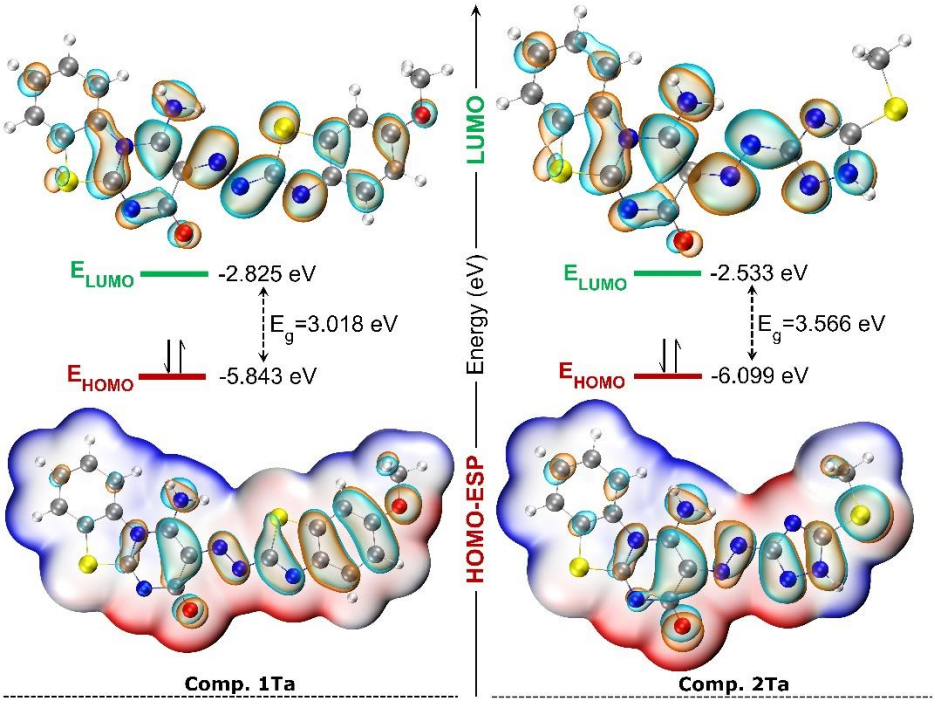

Figure 6. ESP-HOMO and LUMO surface of the compounds **1** and **2**.

As a result of tautomerization, intramolecular interactions and hydrogen bonds are formed. In **Figure 7**, IRI surfaces showing intramolecular interactions of tautomer **1Ta** are given. In addition, QTAIM calculations give charge densities in RCPs and BCPs (see **Figure 8**). IRI surfaces can also be used to visualize interatomic bond electron densities. As seen in **Figure 7**, N=N bond (B9, π-bond) and C–C (B6, σ-bond) had distinctly different surfaces in terms of electron density (darker red indicates higher electron density). It was observed that NH_2 and NH structures on the pyrimidine ring of tautomers make strong intramolecular hydrogen bonds.

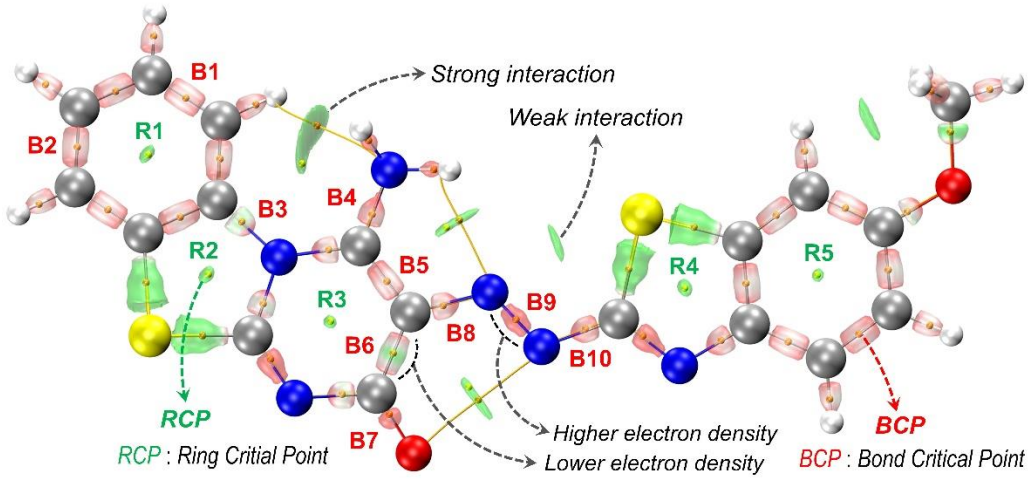

Figure 7. IRI surface of intramolecular interaction and QTAIM points of compound **1Ta**.

Considering that the hydrogen atoms around the central nitrogen atoms in tautomeric structures make high contributions to the intramolecular interactions, it can be said that the B1, B2 and B3 bonds cause the electron densities in BCPs not to be affected much by tautomerization (see **Figure 8**). B4 has a sigma bond only in **Ta**-type taoutomers and it can be seen from the IRI and QTAIM data that the bond electron density increases due to the =NH bond structure (π-bond) in other tautomers. The bond electron densities of **Td** tautomers vary more than those of other tautomers, and the calculated total energies of both **1Td** and **2Td** are higher than other tautomers in their group. **Tc** tautomers with both NH⋯N and NH⋯O interactions have lower molecular energy (in the gas phase, for **1T**(**a-d**): -1968.839, -1968.858, -1968.863, and -1968.827, a.u, respectively; for **2T**(**a-d**): -1811.326, -1811.3376, -1811.3496, and -1811.3026 a.u, respectively). Electron densities in RCPs are not affected by tautomerization and are generally calculated around 0.023 *e*/bohr^3 at R1, R3 and R5 points, and around 0.038 and 0.043/0.063 e/bohr3 for compound **1** and **2** tautomers at R2 and R4 points, respectively.

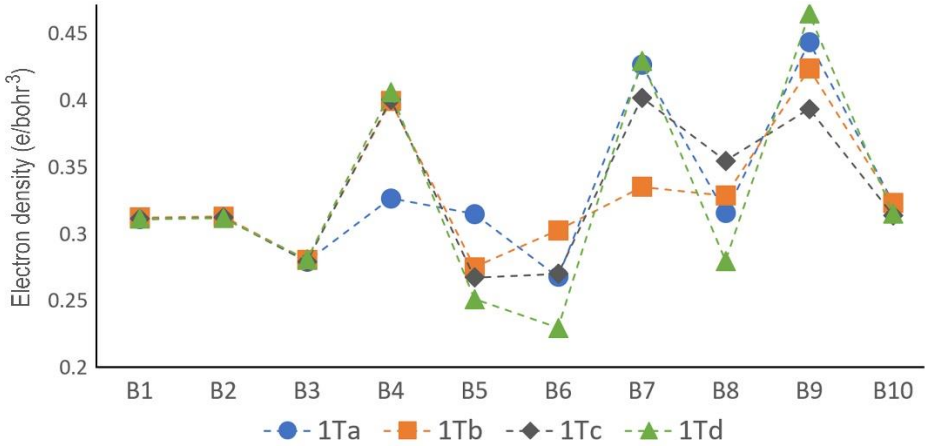

Figure 8. Electron density values (*e*/bohr^3) on the BCPs of the tautomers.

UV calculations of the tautomers were performed at the B3LYP/6-311++G(2d,2p) theory level in the same solvent phase as the experiments. In general, it was observed that the absorption peaks were not affected by the change of solvents (**Table 5**; **Figure 9-a,b**). It was observed that the 2-amino-6-methoxy benzothiazole moiety shifted the absorption peaks to higher wavelengths compared to 3-amino-5-metil-tiyo-1H-1,3,4-triazol moiety. That is, the maximum absorption wavelengths of the tautomers of compound **1** were

calculated larger than those of the tautomers of compound **2**. In the similar tautomeric conformations of compounds **1** and **2**, the maximum absorption peak of the **Tb** isomer shifted to higher wavelengths, while in **Td** it shifted to lower wavelengths. Considering that electrons in transit from HOMO to LUMO in general are responsible for the maximum absorption peaks, it is an expected result that tautomers with small E_g values will give absorption peaks at higher wavelengths. In addition, tautomers **Tb** and **Tc** showing absorption peak curves close to each other may be due to the similar characteristics of intramolecular hydrogen bonds.

Table 5. Calculated UV data (absorption values > 300 nm)

Isomer	Acetic acid	Acetonitrile	DMF	DMSO	Chloroform	Methanol
1 Ta	470, 331	471, 331	474, 332	474, 332	472, 331	470, 331
1Tb	531	531	535	535	534	530
1Tc	504, 315	504, 316	507, 316	507, 316	505, 316	504, 316
1Td	413, 329s	415, 330	417, 330	417, 330	413, 321s	415, 330
2 Ta	403, 333	405, 340	407, 341	406, 341	404, 333	405, 340
2Tb	429, 320	430, 323	432, 323	431, 324	430, 318	429, 323
2Tc	428, 327	431, 329	433, 330	432, 330	428, 326	431, 329
2Td	331	332	333	333	331	332

s: shoulder.

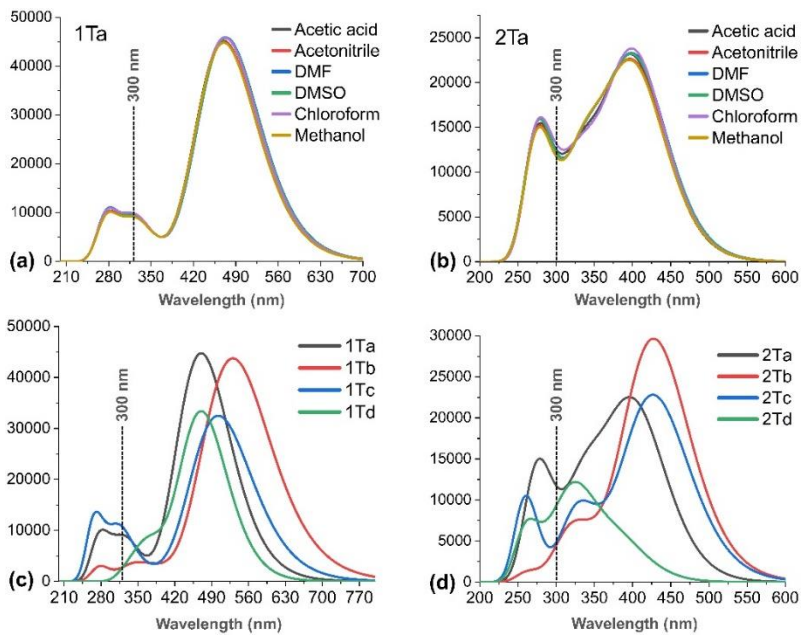

Figure 9. UV data of tautomers. (a) and (b): UV absorption plots of 1Ta and 2Ta tautomers in different solvents, (c) and (d): UV absorption graphs of **1** and **2** tautomers in methanol solvent.

4. Conclusion

Four different possible tautomer structures are contemplated for each of the compounds. Parallel to the experimental spectral studies, calculations were performed at the level of B3LYP/6-311++G(2d,2p) and data to support the experimental results were obtained.

The relationship between the tautomeric structures of the compounds and their electronic properties was investigated theoretically. The effects of tautomeric transitions on the conformational and spectral properties of the compounds have been demonstrated. The calculations led to the prediction that the first group tautomers containing 2-amino-6-methoxy benzothiazole may be more reactive than the second group tautomers containing 3-amino-5-methyl-thio-1H-1,3,4-triazole, since the first group tautomers are more electrophilic, have higher polarizability and electron accept-donor power, and also have lower Eg values.
It was determined that tautomerization can form intramolecular interactions and hydrogen bonds, and tautomers with intramolecular hydrogen bonds such as NH⋯N and NH⋯O have lower molecular energy. It has also been shown that IRI surfaces can be used to visualize interatomic bond electron densities.

It was observed that the absorption peaks were not affected by the solvent change. In addition, it was observed that the 2-amino-6-methoxy benzothiazole moiety decreased the Eg value compared to the 3-amino-5-methyl-thio-1H-1,3,4-triazole group and, in parallel, shifted the absorption peaks to higher wavelengths.he template file. The text under this heading should be Times News Roman-12 points.

Authorship contribution statement

N. Şener: Synthesis and characterization, Investigation, Resource/Material/Instrument Supply.

M. S. Çavuş: Conceptualization, Methodology, Theoretical Calculations, Formal, Analysis, Investigation, Visualization.

Declaration of competing interest

As the authors of this study, we declare that we do not have any conflict of interest statement.

Acknowledgment

The authors are grateful to the Scientific Research Projects Council of Kastamonu University (KÜ-BAP01/2019-9). The DFT calculations reported in this paper were partially performed at TUBITAK ULAKBIM, High Performance and Grid Computing Center (TRUBA resources).

Ethics Committee Approval and/or Informed Consent Information

As the authors of this study, we declare that we do not have any ethics committee approval and/or informed consent statement.

References

[1] H. Zollinger, “Color chemistry: Syntheses, Properties and Application of Organic, Dyes and Pigments” 2nd ed. Weinheim: VCH; 1991.
[2] P. I. Gregory and K. Hunger, “Industrial Dyes: Chemistry, Properties and Applications”, Weinheim: Wiley-VCH, 2002,pp.543–585.
[3] R. J. H. Clark and R. E. Hester, “Advances In Materials Science Spectroscopy”. New York:John Wiley & Sons; 1991.
[4] M. Neamtu, A. Yediler, I. Siminiceanu, M. Macoveanu and A. Kettrup, “Decolorization of disperse red 354 azo dye in water by several oxidation processes - a comparative study,” *Dyes and Pigments*, 60 (1), 61-68, 2004.
[5] A. Akbari, J. C. Remigy and P. Aptel, “Treatment of textile dye effluent using a polyamide-based nanofiltration membrane,” *Chemical Engineering and Processing*, 41 (7), 601-609, 2002.

[6] J. Geng, T. Tao, S. J. Fu, W. You and W. Huang, "Structural investigations on four heterocyclic Disperse Red azo dyes having the same benzothiazole/azo/benzene skeleton," *Dyes and Pigments*, 90 (1), 65-70, 2011.
[7] A. D. Towns, "Developments in azo disperse dyes derived from heterocyclic diazo components," *Dyes and Pigments*, 42, 3–28, 1999.
[8] M. R. Maliyappa, J. Keshavayya, N. M. Mallikarjuna, P. M. Krishna, N. Shivakumara, T. Sandeep and M. A. Nazrulla, "Synthesis, characterization, pharmacological and computational studies of 4, 5, 6, 7-tetrahydro-1, 3-benzothiazole incorporated azo dyes," *Journal of Molecular Structure*, 1179, 630-641, 2019.
[9] B. N. Ravi, J. Keshavayya and N. M. Mallikarjuna, "Synthesis, spectral characterization and pharmacological evaluation of Ni (II) complexes of 6-nitro-benzothiazole incorporated azo dyes," *Journal of Inorganic and Organometallic Polymers and Materials*, 30 (9), 3781-3796, 2020.
[10] C. W. Ghanavatkar, V. R. Mishra, N. Sekar, E. Mathew, S. S. Thomas and I. H. Joe, "Benzothiazole pyrazole containing emissive azo dyes decorated with ESIPT core: linear and nonlinear optical properties, Z scan, optical limiting, laser damage threshold with comparative DFT studies," *Journal of Molecular Structure*, 1203, 127401, 2020.
[11] S. Prakash, G. Somiya, N. Elavarasan, K. Subashini, S. Kanaga, R. Dhandapani and V. Sujatha, "Synthesis and characterization of novel bioactive azo compounds fused with benzothiazole and their versatile biological applications," *Journal of Molecular Structure*, 1224, 129016, 2021.
[12] V. R. Mishra, C. W. Ghanavatkar, S. N. Mali, S. I. Qureshi, H. K. Chaudhari and N. Sekar, "Design, synthesis, antimicrobial activity and computational studies of novel azo linked substituted benzimidazole, benzoxazole and benzothiazole derivatives," *Computational biology and chemistry*, 78, 330-337, 2019.
[13] A. S. Özen, P. Doruker & V. Aviyente, "Effect of cooperative hydrogen bonding in azo− hydrazone tautomerism of azo dyes," *The Journal of Physical Chemistry A*, 111 (51), 13506-13514, 2007.
[14] M. R. Maliyappa, J. Keshavayya, M. Mahanthappa, Y. Shivaraj and K. V. Basavarajappa, "6-Substituted benzothiazole based dispersed azo dyes having pyrazole moiety: synthesis, characterization, electrochemical and DFT studies," *Journal of Molecular Structure*, 1199, 126959, 2020.
[15] S. Kınalı, S. Demirci, Z. Çalışır, M. Kurt and A. Ataç, "DFT, FT-IR, FT-Raman and NMR studies of 4-(substituted phenylazo)-3, 5-diacetamido-1H-pyrazoles," *Journal of Molecular Structure*, 993 (1-3), 254-258, 2011.
[16] C. W. Ghanavatkar, V. R. Mishra, S. N. Mali, H. K. Chaudhari and N. Sekar, "Synthesis, bioactivities, DFT and in-silico appraisal of azo clubbed benzothiazole derivatives," *Journal of Molecular Structure*, 1192, 162-171, 2019.
[17] S. Harisha, J. Keshavayya, S. M. Prasanna and H. J. Hoskeri, "Synthesis, characterization, pharmacological evaluation and molecular docking studies of benzothiazole azo derivatives," *Journal of Molecular Structure*, 1218, 128477, 2020.
[18] B. Manjunatha, Y. D. Bodke, O. Nagaraja, G. Nagaraju and M. A. Sridhar, "Coumarin-benzothiazole based azo dyes: synthesis, characterization, computational, photophysical and biological studies," *Journal of Molecular Structure*, 1246, 131170, 2021.
[19] M. R. Maliyappa, J. Keshavayya, M. S. Sudhanva and I. Pushpavathi, "Heterocyclic azo dyes derived from 2-(6-chloro-1, 3-benzothiazol-2-yl)-5-methyl-2, 4-dihydro-3H-pyrazol-3-one having benzothiazole skeleton: synthesis, structural, computational and biological studies," *Journal of Molecular Structure*, 1247, 131321, 2022.
[20] M. R. Maliyappa, J. Keshavayya, M. Mahanthappa, Y. Shivaraj, K.V. Basavarajappa, "6-Substituted benzothiazole based dispersed azo dyes having pyrazole moiety: Synthesis, characterization, electrochemical and DFT studies", Journal of Molecular Structure, 1199, 126959, 2020.
[21] C. W. Ghanavatkar, V. R. Mishra, N. Sekar, E. Mathew, S. Sijo Thomas, I. H. Joe, "Benzothiazole pyrazole containing emissive azo dyes decorated with ESIPT core: Linear and nonlinear optical properties, Z scan, optical limiting, laser damage threshold with comparative DFT studies", Journal of Molecular Structure, 1203, 127401, 2020.
[22] M. Gökalp, T. Tilki, Ç. Karabacak Atay, "Newly Synthesized Aminothiazole Based Disazo Dyes and Their Theoretical Calculations", Polycyclic Aromatic Compounds, 1(23), 2023.
[23] S. Erişkin, N. Şener, S. Yavuz and İ. Şener, "Synthesis, characterization, and biological activities of 4-imino-3-arylazo-4H-pyrimido[2, 1-b][1, 3]benzothiazole-2-oles," *Medicinal Chemistry Research*, 23 (8), 3733-3743, 2014.
[24] P. Hohenberg and W. Kohn, *Phys. Rev*., 1964, 136, 864-871.
[25] W. Kohn and L. J. Sham, *Phys. Rev*., 1965, 140, 1133-1138.
[26] M. J. Frisch, G. Trucks, H. Schlegel, G. Scuseria, M. Robb, J. Cheeseman, G. Scalmani, V. Barone, B. Mennucci and G. Petersson, *Inc.: Wallingford*, CT, 2009.
[27] R. F. Bader, *Acc. Chem*. Res., 1985, 18, 9-15.
[28] R. F. Bader, *Chem. Rev*., 1991, 91, 893-928.

[29] Tian Lu and Qinxue Chen, "Interaction Region Indicator: A Simple Real Space Function Clearly Revealing Both Chemical Bonds and Weak Interactions," *Chemistry—Methods*, 1 (5), 231-239, 2021.
[30] T. Lu and F. Chen, J. *Comput. Chem*., 2012, 33, 580-592.
[31] M. R. Maliyappa, J. Keshavayya, R. A. Shoukat Ali and S. Harisha, "Synthesis, Characterization, Solvatochromic and Biological studies of novel Benzothiazole based azo dyes," *Journal of Chemical and Pharmaceutical Sciences*, Special Issue 1 (10-15), 2018.